

Supporting information for 'Resonant light scattering spectroscopy of gold, silver and gold-silver alloy nanoparticles and optical detection in microfluidic channels'

Julien R. G. Navarro^{1,2} and Martinus H. V. Werts^{1,2*}

¹*Ecole Normale Supérieure de Cachan-Bretagne, SATIE (UMR 8029), Campus de Ker Lann, F-35170 Bruz, France.*

²*CNRS, SATIE (UMR 8029), ENS Cachan-Bretagne, Campus de Ker Lann, F-35170 Bruz, France.*

*corresponding author. E-mail : martinus.werts@bretagne.ens-cachan.fr

Contents

1	Transmission electron microscopy of synthesised nanoparticles.	2
1.1	Gold nanoparticles.....	2
1.2	Silver nanoparticles.....	3
1.3	Gold-silver alloy nanoparticles.....	4
2	Rayleigh scattering of dilute Ludox suspension.....	5
3	UV-visible absorption spectroscopy of the reversible aggregation of thioctic acid-capped gold nanoparticles.....	6
4	Mie calculations of light extinction and scattering by gold and silver nanoparticles.....	7
4.1	Size-dependence of the extinction coefficient for gold and silver nanoparticles.....	7
4.2	Light scattering: Mie results.....	11
4.3	Python code for Mie calculations.....	14
	References (SI).....	18

1 Transmission electron microscopy of synthesised nanoparticles

1.1 Gold nanoparticles

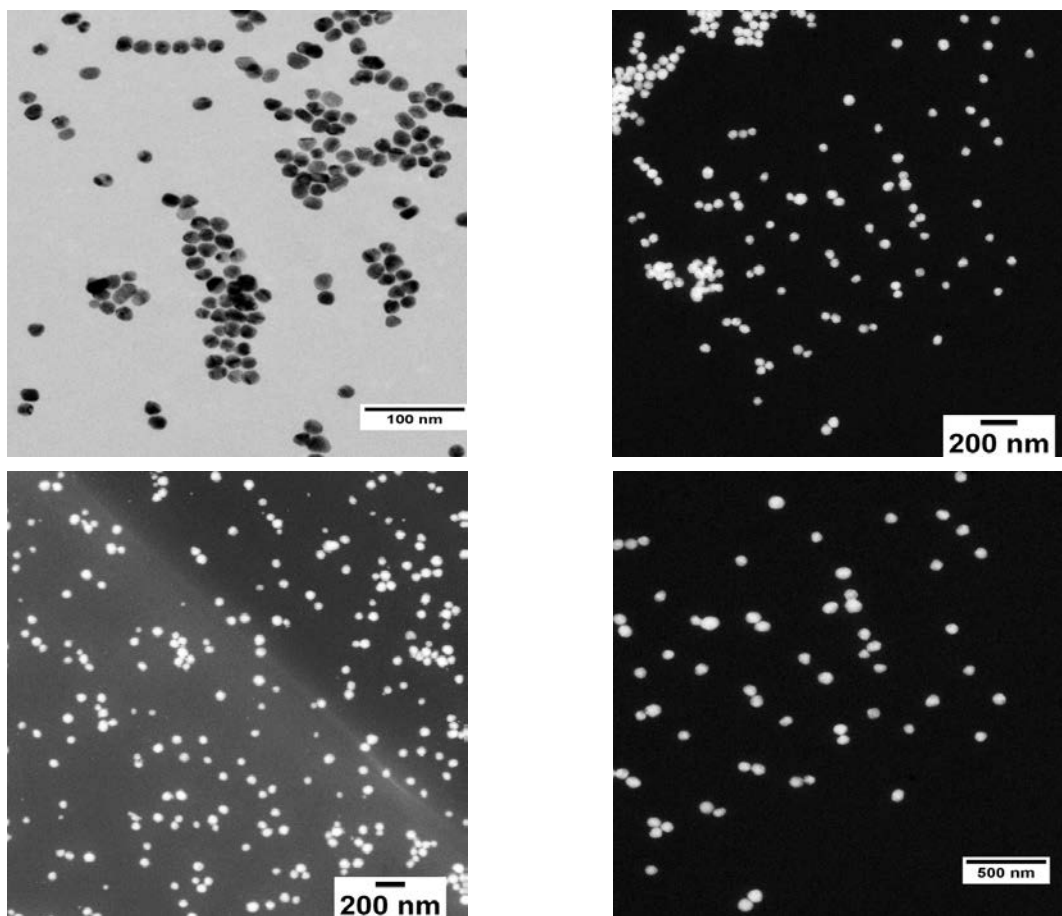


Figure S1. TEM images of gold nanoparticles of different sizes. Top: Au-14nm-TEG (left), Au-54nm-TEG (right). Bottom: Au-75nm-TEG (left), Au-100nm-TEG (right).

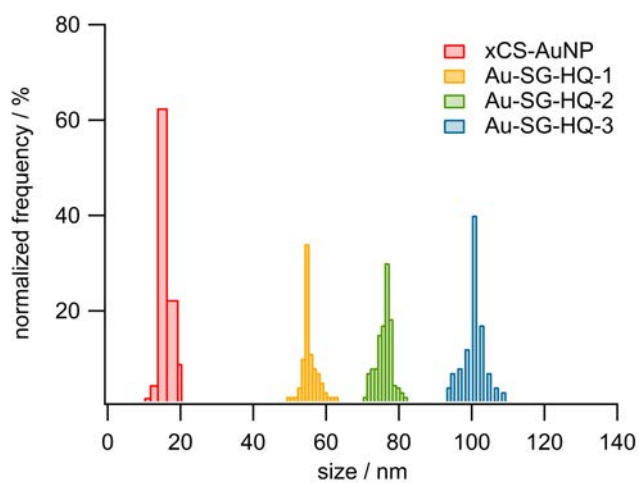


Figure S2. Core size distribution of gold nanoparticles (cf. Figure S1) of different sizes, 14(\pm 2) nm, 54 (\pm 3)nm, 75(\pm 3) nm and 100(\pm 10) nm.

1.2 Silver nanoparticles

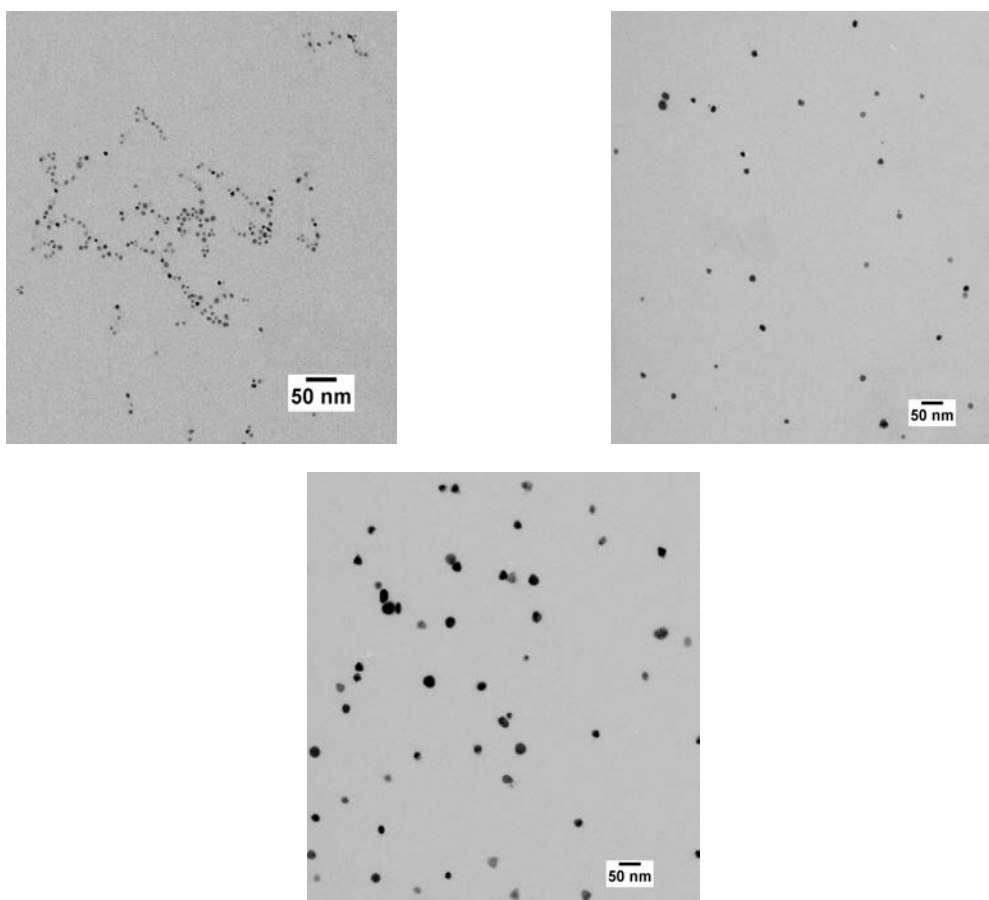


Figure S3. TEM images of silver nanoparticles of different sizes. Top: Ag-5nm-TEG (left), Ag-12nm-TEG (right). Bottom: Ag-18nm-TEG

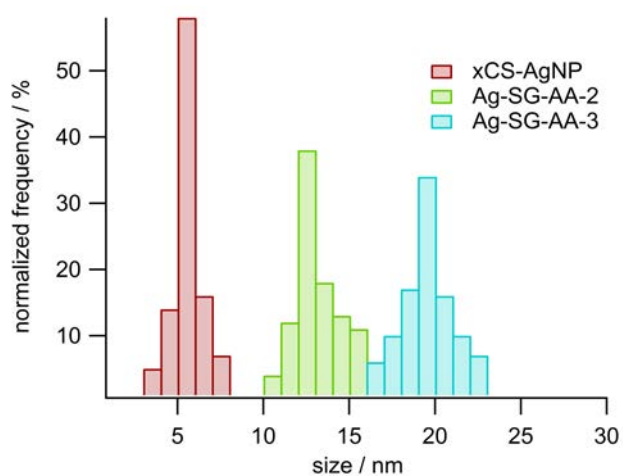


Figure S4. Core size distribution of silver nanoparticles of different sizes (cf. Figure S3): $5.0(\pm 1.5)$ nm, $12(\pm 2)$ nm and $18(\pm 3)$ nm.

1.3 Gold-silver alloy nanoparticles

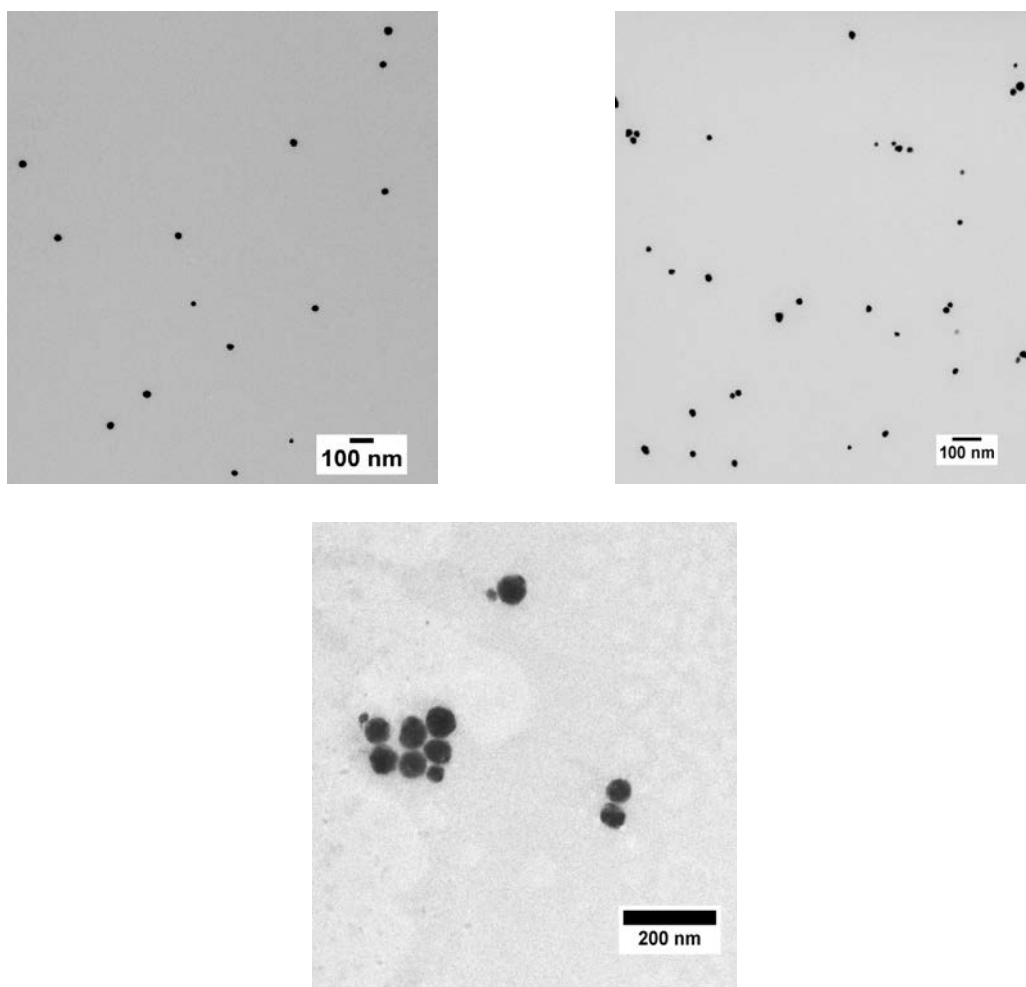


Figure S5. TEM images of silver-gold alloy nanoparticles of different sizes. Top: $\text{Au}_{0.80}\text{Ag}_{0.20}$ -23nm-TEG (left), $\text{Au}_{0.54}\text{Ag}_{0.46}$ -47nm-TEG (right). Bottom: $\text{Au}_{0.27}\text{Ag}_{0.73}$ -61nm-TEG

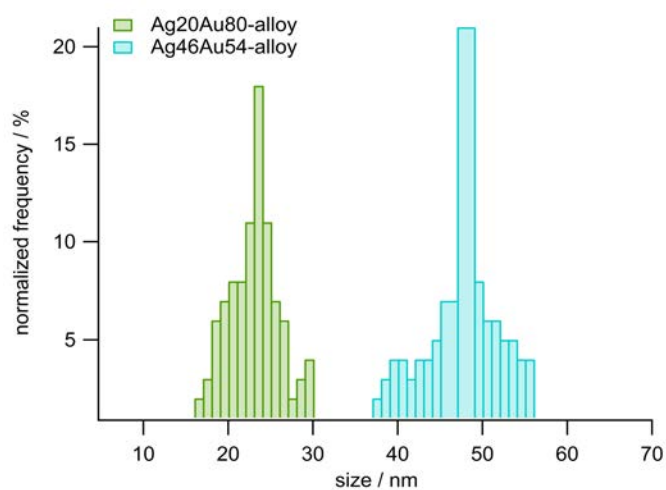


Figure S6. Core size distribution of silver-gold alloy nanoparticles of different sizes (cf. Figure S5): 23(\pm 3) nm ($\text{Au}_{80}\text{Ag}_{20}\text{TEG}$), 47(\pm 7) nm ($\text{Au}_{54}\text{Ag}_{47}\text{TEG}$).

2 Rayleigh scattering of dilute Ludox suspension

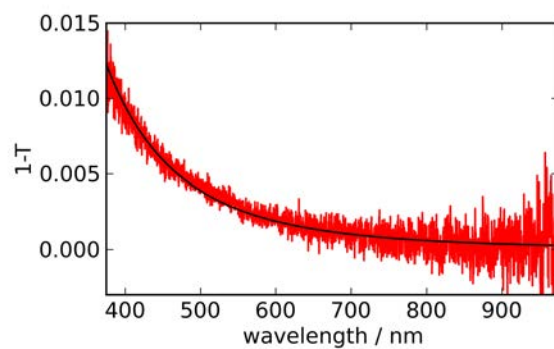


Figure S7. Extinction spectrum (1-transmittance *vs* wavelength) of a suspension of Ludox SM30 diluted in 50mM NaCl (1:200 v/v). Red is the measured spectrum, the black line is the theoretical λ^{-4} dependence for a perfect Rayleigh scatterer.

3 UV-visible absorption spectroscopy of the reversible aggregation of thioctic acid-capped gold nanoparticles

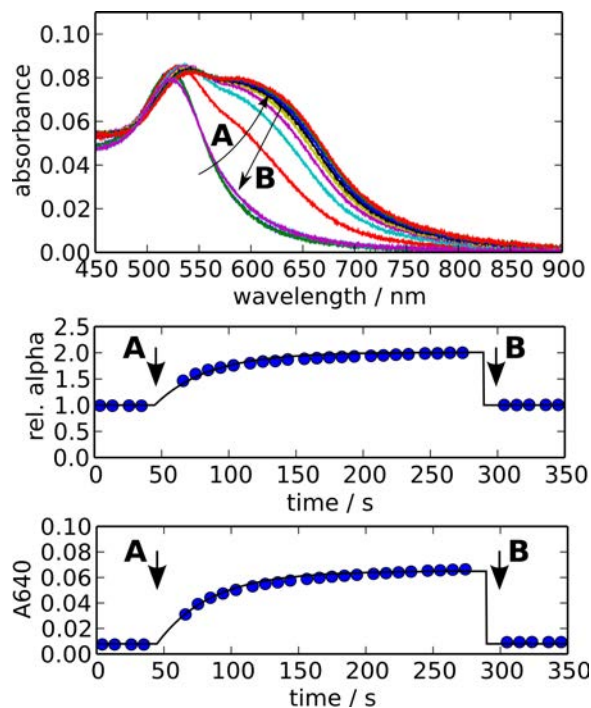


Figure S8. Reversible modulation of the UV-visible absorbance of a suspension of thioctic-acid capped 20 nm gold particles. Initially the particles are in 1mM NaOH (pH 11). At A, the solution is acidified to pH 3 by adding HCl(aq). At B, the pH is brought back by to pH 11 by adding NaOH(aq). Top: UV-visible absorbance of the suspension in a 1 cm cuvette. Middle: average absorbance (α , Equation 9). Bottom: The absorbance at 640 nm (near the maximum of the aggregation-related extinction band) as a function of time. The solid lines are merely a guide to the eye, the data points are blue circles. The AuTA nanoparticle concentration is 9×10^{-11} M.

4 Mie calculations of light extinction and scattering by gold and silver nanoparticles

Here we include results and insights that simple Mie calculations yield concerning extinction coefficients and light scattering properties of gold and silver nanoparticles. The extinction spectrum of gold nanoparticles in solution has already well been studied using Mie calculations,^{S1,S2} but silver has received less attention. The light scattering parameters of metal nanoparticles relevant to the present work are difficult to extract from existing literature, which prompted us to carry out Mie calculations.

The Mie calculations were implemented in Python (with the Scipy and Numpy libraries) based on MATLAB code by Mätzler^{S3}. For the dielectric functions of gold and silver we used the data by Johnson & Christy^{S4}, with the application of the mean-free path correction for small particles as explained for example by Haiss et al.^{S1} This latter correction is mainly significant for particles < 20 nm.

4.1 Size-dependence of the extinction coefficient for gold and silver nanoparticles

Here, we compare the results of Mie calculations with available experimental data concerning the molar extinction coefficients for gold and silver nanoparticles. One particular aim is to obtain simple power-law expressions for the dependence of the maximum extinction coefficient on particle diameter, *i.e.*

$$\epsilon_{\max} = Ad^{\gamma}$$

4.1.1 Gold nanoparticles

Fitting this power law to experimental data for gold nanoparticles, Liu et al.⁵ found $A = 4.93 \times 10^4 \text{ M}^{-1} \text{ cm}^{-1}$ and $\gamma = 3.32$ with d the diameter in nanometers. The coefficients were later slightly refined^{S6} to be $A = 4.60 \times 10^4 \text{ M}^{-1} \text{ cm}^{-1}$ and $\gamma = 3.34$, by inclusion of further data from the literature. The combined experimental data for this fit spans only particles diameters between 5 and 35 nm. Here, we add additional experimental points using commercially supplied gold nanoparticles and the accurate particle concentration supplied by the manufacturer. We plotted the experimental data points (Figure S9), together with the results of Mie calculations (see below).

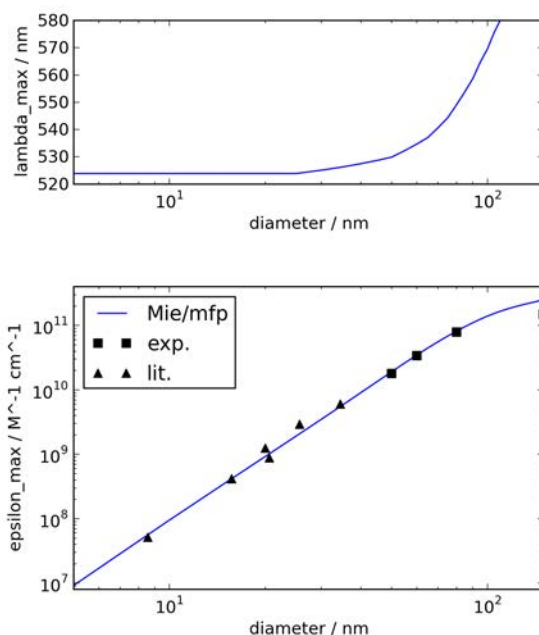


Figure S9. Extinction data for gold nanoparticles in water ($n = 1.33$). Top: Position of longest wavelength maximum of the extinction spectrum, as a function of particle diameter, from Mie calculations. Bottom: corresponding extinction coefficient from Mie calculations (blue line), compared to experimental data from literature (triangles) and from this work (squares).

The Mie calculations very reliably reproduce the experimental data points, as has already been reported for gold nanoparticles^{S1,S2}. However, the results of Mie calculations reported by Yguerabide and Yguerabide⁷ seem to systematically overestimate the extinction coefficients compared to both the experimental data and the present Mie calculations.

In order to obtain a simple power-law expression for the maximum extinction coefficient as a function of gold nanoparticle diameter we fit power laws to the results from Mie calculations (Figure S10). Two regimes were identified, with a transition around 85 nm.

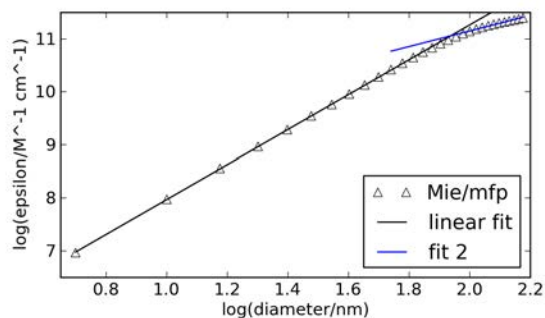


Figure S10. Power law behaviour of the extinction coefficient as a function of particle diameter for gold nanoparticles. Triangles: the results of individual Mie calculations (mean free path corrected). The black and blue lines are the power-law fits for smaller (<85 nm) and bigger (>85 nm) nanoparticles.

This fit yields $A = 4.7 \times 10^4 \text{ M}^{-1} \text{ cm}^{-1}$ and $\gamma = 3.30$. These coefficients can reliably be used to predict extinction coefficients for particles with diameters between 5 and 85 nm. Between 85 nm and 150 nm, a satisfactory description is given by $A = 1.6 \times 10^8 \text{ M}^{-1} \text{ cm}^{-1}$ and $\gamma = 1.47$. All these results refer to water as the medium ($n=1.33$).

$$\epsilon_{\text{max}}^{\text{gold}} = Ad^{\gamma} \begin{cases} A=4.7 \times 10^4 \text{ M}^{-1} \text{ cm}^{-1}, \gamma=3.30, d \leq 85 \text{ nm} \\ A=1.6 \times 10^8 \text{ M}^{-1} \text{ cm}^{-1}, \gamma=1.47, d > 85 \text{ nm} \end{cases}$$

4.1.2 Silver nanoparticles

Data and systematic calculations for silver nanoparticles are more scarce, and it is therefore interesting to compare published experimental data with the results from Mie calculations. Such comparisons are not readily found in literature. Evanoff and Chumanov reported useful experimental measurements of the extinction coefficients of silver nanoparticles for a range of sizes.⁵⁸ The agreement between the results from Mie calculations and the experimental data is not very good (Figure S11), although the general trend and the orders of magnitude are confirmed

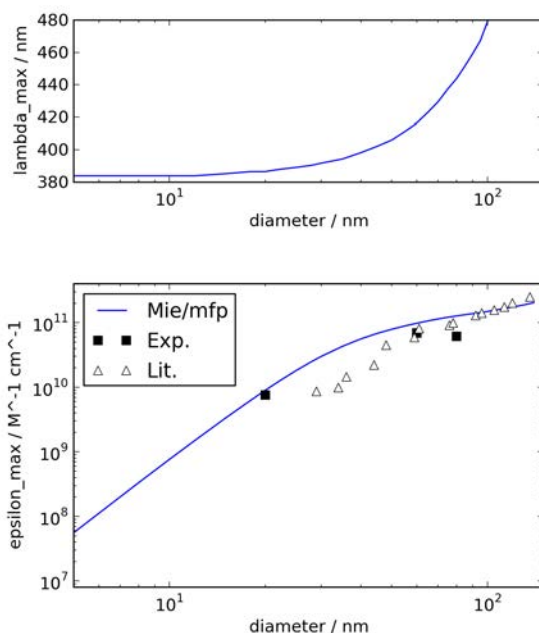


Figure S11. Extinction data for silver nanoparticles in water ($n = 1.33$). Top: Position of longest wavelength maximum of the extinction spectrum, as a function of particle diameter, from Mie calculations. At larger particle sizes a quadrupolar resonance appears at short wavelengths, whose peak extinction coefficient is larger, but this band is ignored. Bottom: corresponding extinction coefficient from Mie calculations (blue line), compared to experimental data from literature (triangles) and from this work (squares).

The optical response of silver is much more sensitive to surface effects. In combination with the propensity of silver to be more readily oxidised, this may explain the deviation of the experimental results from the idealised particles that are calculated using theory. It is likely that Mie calculations are actually most reliable guide for silver nanoparticles, provided that perfectly spherical, monodisperse particles are obtained. Therefore, we will use a power-law fit to the Mie data for an estimation of the extinction coefficient of silver nanoparticles (Figure S12).

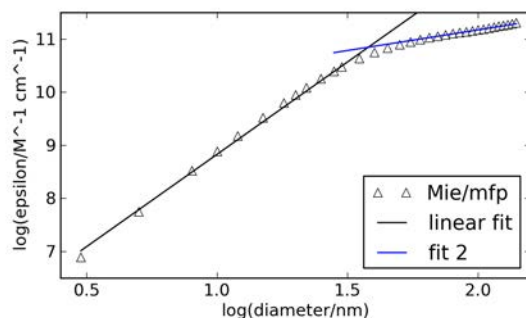


Figure S12. Power law behaviour of the extinction coefficient as a function of particle diameter for silver nanoparticles. Triangles: the results of individual Mie calculations (mean free path corrected). The black and blue lines are the power-law fits for smaller (<38 nm) and bigger (>38 nm) nanoparticles.

In absence of more experimental data from independent sources, we will for now estimate extinction coefficients for silver nanoparticles in water using the following (Mie-theory based) power-law.

$$\epsilon_{\max}^{\text{silver}} = Ad^{\gamma} \begin{cases} A=2.3 \times 10^5 \text{ M}^{-1} \text{ cm}^{-1}, \gamma=3.48, d \leq 38 \text{ nm} \\ A=4.2 \times 10^8 \text{ M}^{-1} \text{ cm}^{-1}, \gamma=0.77, d > 38 \text{ nm} \end{cases}$$

4.2 Light scattering: Mie results

Quantitative data of the light scattering properties were also obtained through Mie calculations, as exemplified by the spectra in Figure S13. The RLS scattering spectra are expressed as the ratio Q_{sca} of the scattering cross section σ_{sca} and the physical cross section $\pi(d/2)^2$. For suitably sized gold and silver nanoparticles, the (optical) scattering cross sections exceed their physical cross sections (for comparison, organic fluorophores have photoluminescence action cross section that are at best 5% of their physical cross section).

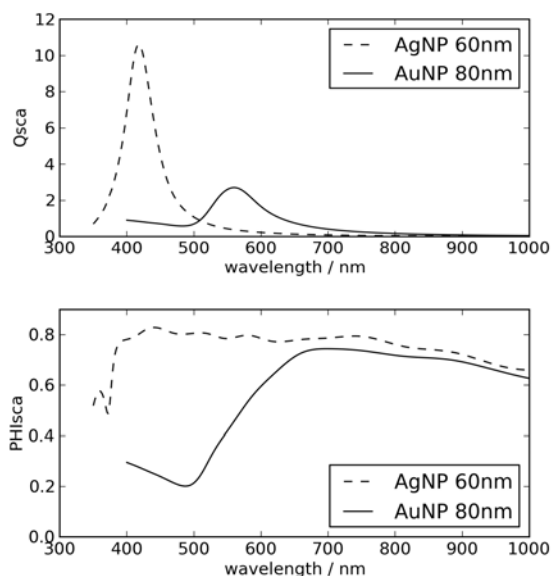


Figure S13. Calculated scattering spectra for larger silver (60 nm) and gold (80 nm) nanoparticles in water. Top: spectra represented as the ratio of scattering cross section to the physical cross section. Bottom: wavelength-dependence of the scattering efficiency for these particles.

The scattering efficiency $\varphi_{\text{sca}}(\lambda)$ was calculated according to Eqn. 3 (main text), the ratio of scattering and total extinction cross sections (Figure S13, bottom). Especially in the case of gold nanoparticles, this efficiency depends on wavelength.

A representative overall value for the scattering efficiency (Φ_{sca}) can be obtained by Eqn. 5. The spectral region of interest chosen was 400-900 nm. The diameter-dependence of this overall cross section is displayed in Figure S14. Interestingly, these values do not differ much from the value of φ_{sca} at the plasmon maximum wavelength. The evolution of the scattering efficiency as a function of diameter is plotted in Figure S14.

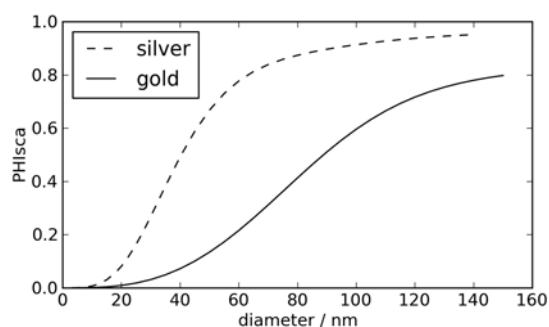


Figure S14. Calculated overall (400-900 nm) scattering efficiencies as a function of diameter for gold and silver nanoparticles in water.

The angular distribution of scattered light is of interest for the right-angle, reference-based scattering efficiency measurement described in the main text. This distribution can also be obtained through application of Mie calculations. One relevant parameter that gives some insight is the so-called asymmetry parameter, which is the average value of the cosine of the scattering angle, which can vary between -1 and 1. For very small particles, such as Ludox, this value is zero. Deviations from zero may be interpreted as changes in the angular distribution.

In our calculations we find that the asymmetry parameter, while not completely zero, remains small even for moderately sized particles (see Figure S15). We therefore expect the right-angle measurements of scattering efficiency to yield useful values for comparing the scattering efficiencies of different types of particles. For future studies it may be interesting to compare efficiencies measured at right-angles to efficiencies measured using an integrating sphere.

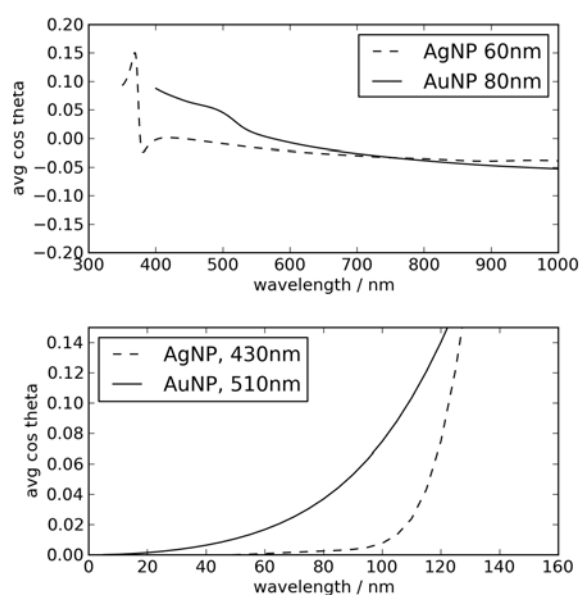


Figure S15. Top: Scattering asymmetry parameter $\langle \cos \theta \rangle$ as a function of wavelength, calculated for 60 nm silver and 80 nm gold nanoparticles. Bottom: Evolution of the asymmetry parameter at a characteristic wavelength as a function of diameter, for gold and silver nanoparticles in water.

4.3 Python code for Mie calculations

The Mie calculations, based on the MATLAB code by Mätzler⁵³, were implemented in Python, with the Scipy, Numpy and Matplotlib libraries. We used the 64-bit Enthought Python Distribution 7.2 (Enthought Inc., Austin TX, USA), but the code will also run on standard distributions (Python 2.7.2 with Scipy 0.10.0, Numpy 1.6.1, Matplotlib 1.1.0). Here we only give the main calculation code, which exports the calculated spectra for different particle diameters to an output file for subsequent processing and data extraction. As with the original MATLAB code, all computation intensive operations are vectorised and carried out by dedicated routines, in Python provided by the Numpy/Scipy libraries (which rely on compiled C and FORTRAN routines). This keeps the calculations fast, in spite of Python – like MATLAB - being an interpreted language.

```
from pylab import *
from scipy import special
from scipy import interpolate
import cPickle

# CALCULATION PARAMETERS

# name of result pickle file
resultfp = 'Mie-result-gold-mfp.pkl'

# materials definition
mat = 'Au' # definition of the material gold='Au', silver='Ag'
n_medium = 1.33 # water

# list of diameters to be calculated
# in meters
list_diam=array([ 5,10,15,20,25,30,35,40,45,50,55,60,65,70,75,80,85,90,
                 95,100,105,110,115,120,125,130,135,140,145,150])*1e-9

# spectra specifications
specstart = 400e-9 # wavelengths in meters
specend = 1000e-9
Npts_spectrum = 500 # number of points in a spectrum

# FUNCTION DEFINITIONS

# definition of Mie routines Mie_abcd and Mie
def Mie_abcd(m, x, nmax):
    """based on the MATLAB code by C. Maetzler, 2002
    Ref.: (Maetzler 2002)
    """
    n = arange(1, (nmax+1))*1.0
    nu = n+0.5
    z = m*x
    m2 = m*m
    sqx = sqrt(0.5 * pi / x)
    sqz = sqrt(0.5 * pi / z)

    bx = special.jv(nu, x) * sqx
    bz = special.jv(nu, z) * sqz
    yx = special.yv(nu, x) * sqx
    hx = (complex(1,0)*bx + complex(0,1)*yx)

    blx = concatenate((array([(sin(x)/x)]),bx[0:(nmax-1)]))
    blz = concatenate((array([(sin(z)/z)]),bz[0:(nmax-1)]))
    ylx = concatenate((array([(-cos(x)/x)]),yx[0:(nmax-1)]))
```

```
hlx = complex(1,0)*b1x + complex(0,1)*y1x

ax = x*b1x - n*bx
az = z*b1z - n*bz
ahx = x*hlx - n*hx

an = (m2*bz*ax - bx*az)/(m2*bz*ahx - hx*az)
bn = (bz*ax - bx*az)/(bz*ahx - hx*az)
cn = (bx*ahx - hx*ax)/(bz*ahx - hx*az)
dn = m*(bx*ahx - hx*ax)/(m2*bz*ahx - hx*az)

return (an,bn,cn,dn)

def Mie(m, x):
    """The Mie routine adapted from Maetzler MATLAB code (Maetzler 2002).
    It calculates extinction, scattering and absorption cross sections, as well as
    the asymmetry parameter (avg cos theta)
    for a single value of x, based on the complex refractive index contrast m.
    See the Maetzler document for the definition of x and m.
    The result is returned in the form of a 'tuple'.
    Not all properties calculated in the original code are calculated here
    (partial implementation).
    """
    # check x==0 and avoid singularity
    if x==0:
        return (m.real, m.imag, 0., 0., 0., 0., 0.)

    nmax = round(2.0+x+4.0*x**(1./3.))
    n1 = nmax - 1
    n = arange(1,nmax+1)
    cn = 2.0*n + 1.0
    c1n = n*(n+2.0)/(n+1.0)
    c2n = cn/n/(n+1.0)
    x2 = x*x

    (Mie_an,Mie_bn,Mie_cn,Mie_dn)=Mie_abcd(m, x, nmax)
    anp = Mie_an.real
    anpp = Mie_an.imag
    bnp = Mie_bn.real
    bnpp = Mie_bn.imag

    g1=zeros((4,nmax))
    g1[0,0:n1]=anp[1:nmax]
    g1[1,0:n1]=anpp[1:nmax]
    g1[2,0:n1]=bnp[1:nmax]
    g1[3,0:n1]=bnpp[1:nmax]

    dn = cn*(anp+bnp)
    q = sum(dn)
    Qext = 2*q/x2
    en = cn*(anp*anp + anpp*anpp + bnp*bnp + bnpp*bnpp)
    q = sum(en)
    Qsca = 2*q/x2
    Qabs = Qext-Qsca

    asy1 = c1n*(anp*g1[0,:]+anpp*g1[1,:]+bnp*g1[2,:]+bnpp*g1[3,:])
    asy2 = c2n*(anp*bnp + anpp*bnpp)
    asy = 4.0/x2 * sum(asy1+asy2)/Qsca

    # Qb backscatter, Qratio are
    # not calculated here, contrary to original code

    # return results as a tuple
    return (m.real,m.imag,x,Qext,Qsca,Qabs,asy)

def ncmplx_mfpcorr(ncmplx_bulk, radius, waveln, FV, OMP, OM0):
    """mean free path correction
    adapted from Haiss FORTRAN code (Haiss et al. 2007),
    which is in cgs units, which was maintained here
    We used this code with minimal changes
    (this is why there are UPPERCASE variable names...)
    radius, waveln in nanometers
    FV in cm/s, OMP, OM0 in 1E-14 Hz
    """
    rn = ncmplx_bulk.real
    rk = ncmplx_bulk.imag
    CL = 2.998E+10
```

```
# Calculate EPS1 and EPS2 from rn and rk:
EPS1 = rn*rn - rk*rk
EPS2 = 2.*rn*rk
# Calculate OM and A1 and A2:
# CL speed of light in cm/s
OM = (2.*pi*CL/(waveln*1.E-7))/1.E+14
# OMP: bulk plasma frequency in Hz divided by 1E+14
# OM0: collision frequency in Hz/1E+14
A1 = 1.-(OMP*OMP/(OM*OM + OM0*OM0))
A2 = OMP*OMP*OM0/(OM*(OM*OM + OM0*OM0))
# Contribution of the bond electrons to n (B1) and k (B2):
B1 = EPS1 - A1
B2 = EPS2 - A2
# Calculate R dependent OM0 (OM0R)
OM0R = OM0 + (FV/(radius*1.E-7))/1.E+14
# Calculate R dependent contributions of the free electrons:
A1R = 1.-(OMP*OMP/(OM*OM + OM0R*OM0R))
A2R = OMP*OMP*OM0R/(OM*(OM*OM + OM0R*OM0R))
# Calculate R dependent EPS (EPS1R and EPS2R)
EPS1R = A1R + B1
EPS2R = A2R + B2
# Reconvert EPS1R and EPS2R back to n and k:
rnr = sqrt((A1R + B1)/2. + \
           sqrt((A1R/2.+B1/2.)*(A1R/2.+B1/2.)+(A2R/2.+B2/2.)*(A2R/2.+B2/2.)))
rkr = sqrt(-(A1R + B1)/2. + \
           sqrt((A1R/2.+B1/2.)*(A1R/2.+B1/2.)+(A2R/2.+B2/2.)*(A2R/2.+B2/2.)))
# reconstruct complex index
ncmplx_corr = complex(1,0) * rnr + complex(0,1) * rkr
return ncmplx_corr

# complex dielectric functions of gold and silver by Johnson and Christy
if mat == 'Au':
    E = array([0.64,0.77,0.89,1.02,1.14,1.26,1.39,1.51,1.64,1.76,1.88,2.01,2.13,2.26,2.38,2.50,
2.63,2.75,2.88,3,3.12,3.25,3.37,3.5,3.62,3.74,3.87,3.99,4.12,4.24,4.36,4.49,4.61,4.74,4.86,
4.98,5.11,5.23,5.36,5.48,5.6,5.73,5.85,5.98,6.1,6.22,6.35,6.47,6.6])
    n = array([0.92,0.56,0.43,0.35,0.27,0.22,0.17,0.16,0.14,0.13,0.14,0.21,0.29,0.43,0.62,1.04,
1.31,1.38,1.45,1.46,1.47,1.46,1.48,1.50,1.48,1.48,1.54,1.53,1.53,1.49,1.47,1.43,1.38,1.35,
1.33,1.33,1.32,1.32,1.30,1.31,1.30,1.30,1.30,1.30,1.33,1.33,1.34,1.32,1.28])
    k = array([13.78,11.21,9.519,8.145,7.150,6.350,5.663,5.083,4.542,4.103,3.697,3.272,
2.863,2.455,2.081,1.833,1.849,1.914,1.948,1.958,1.952,1.933,1.895,1.866,1.871,1.883,1.898,
1.893,1.889,1.878,1.869,1.847,1.803,1.749,1.688,1.631,1.577,1.536,1.497,1.460,1.427,1.387,
1.350,1.304,1.277,1.251,1.226,1.203,1.188])
    # following values are from Haiss et al.
    FV = 1.4E8 # Fermi velocity in cm/s - needed by mean free path correction
    OMP = 138. # plasma frequency in Hz/1E+14
    OM0 = 0.333 # collision frequency in Hz/1E+14

if mat == 'Ag':
    E = array([0.64,0.77,0.89,1.02,1.14,1.26,1.39,1.51,1.64,1.76,1.88,2.01,2.13,
2.26,2.38,2.50,2.63,2.75,2.88,3,3.12,3.25,3.37,3.5,3.62,3.74,3.87,3.99,4.12,
4.24,4.36,4.49,4.61,4.74,4.86,4.98,5.11,5.23,5.36,5.48,5.6,5.73,
5.85,5.98,6.1,6.22,6.35,6.47,6.6])
    n = array([0.24,0.15,0.13,0.09,0.04,0.04,0.04,0.04,0.03,0.04,0.05,0.06,0.05,
0.06,0.05,0.05,0.05,0.04,0.04,0.05,0.05,0.07,0.1,0.14,0.17,0.81,1.13,1.34,
1.39,1.41,1.41,1.38,1.35,1.33,1.31,1.3,1.28,1.28,1.26,1.25,1.22,1.20,1.18,1.15,
1.14,1.12,1.10,1.07])
    k = array([14.08,11.85,10.10,8.828,7.795,6.692,6.312,5.727,5.242,4.838,4.483,
4.152,3.858,3.586,3.324,3.093,2.869,2.657,2.462,2.275,2.07,1.864,1.657,1.419,
1.142,0.829,0.392,0.616,0.964,1.161,1.264,1.331,1.372,1.387,1.393,1.389,1.378,
1.367,1.357,1.344,1.342,1.336,1.325,1.312,1.296,1.277,1.255,1.232,1.212])
    # following values are from Kreibig 1974 + Murata, Tanaka 2010
    FV = 1.4E8 # Fermi velocity in cm/s - needed by mean free path correction
    OMP = 137. # plasma frequency in Hz/1E+14
    OM0 = 0.27 # collision frequency in Hz/1E+14

ncmplx = complex(1,0) * n + complex(0,1) * k # construct complex vector
ncmplx_interpol=interpolate.interpld(E, ncmplx, kind='cubic')

# CALCULATION
list_Qsca=[]
list_Qext=[]
list_epsilon=[]
list_phisca=[]
list_asy=[]
Npts = Npts_spectrum
wvln = linspace(specstart,specend,Npts)
ncmplx_wvln = ncmplx_interpol(1240.0/(1e9*wvln))
```

```
# loop through the list of particles diameters to be examined
# calculate the spectra, and store all results in lists
for idxb,D_part in enumerate(list_diam) :
    r_part = D_part/2.0 # radius is half the diameter!

    # mean-free path corrected indices (vectorial calculation)
    ncmplx_r_wvln = ncmplx_mfpcorr(ncmplx_wvln, r_part*1e9, wvln*1e9, FV, OMP, OMO)

    Qext = zeros(Npts)
    Qsca = zeros(Npts)
    Qabs = zeros(Npts)
    asy = zeros(Npts)
    for idx in xrange(Npts):
        xco = (2*pi*n_medium*r_part)/wvln[idx]
        # m = ncmplx_wvln[idx]/n_medium # use bulk dielectric function
        m = ncmplx_r_wvln[idx]/n_medium # use mean-free path corrected function
        resulttuple = Mie(m, xco)
        Qext[idx] = resulttuple[3]
        Qsca[idx] = resulttuple[4]
        Qabs[idx] = resulttuple[5]
        asy[idx] = resulttuple[6]

    # add Qsca, Qext spectra to list
    list_Qsca.append(Qsca)
    list_Qext.append(Qext)
    list_asy.append(asy)

    # calculate extinction cross sections
    oext = (r_part*r_part)*pi*Qext

    # calculate molar extinction coefficient and scatter efficiency
    epsilon=1/(3.82e-25)*oext
    phisca=Qsca/Qext

    # add extinction coeff and scatter efficiency spectrum for the current particle size to list
    list_epsilon.append(epsilon)
    list_phisca.append(phisca)

output=open(resultfp,'wb')
cPickle.dump(list_diam,output)
cPickle.dump(wvln,output)
cPickle.dump(list_Qext,output)
cPickle.dump(list_Qsca,output)
cPickle.dump(list_epsilon,output)
cPickle.dump(list_phisca,output)
cPickle.dump(list_asy,output)
output.close()

# Literature references
#
# (Maetzler 2002):
# C. Maetzler, "MATLAB Functions for Mie Scattering and Absorption",
# Research Report 2002-08, Institut fuer Angewandte Physik,
# Universitaet Bern, 2002
# downloaded from http://www.iap.unibe.ch/publications/download/201/en/
#
# (Johnson and Christy 1972):
# P.B. Johnson and R.W. Christy, "Optical Constants of the Noble
# Metals", Phys. Rev. B. 1972, (6), 4370
#
# (Haiss et al. 2007):
# W. Haiss, N.T.K. Thanh, J. Aveyard, D.G. Fernig, "Determination of
# size and concentration of gold nanoparticles from UV-vis spectra.",
# Anal. Chem. 2007, (79), 4215
#
# (Kreibig 1974):
# U. Kreibig. "Electronic properties of small silver particles: the
# optical constants and their temperature dependence",
# J. Phys. F: Metal Phys. 1974, 4, 999
#
# (Murata and Tanaka 2010):
# K.I. Murata, H. Tanaka. "Surface-wetting effects on the liquid-liquid
# transition of a single-component molecular liquid.",
# Nature Commun. 2010, 1, 16
```

References (SI)

- S1. W. Haiss, N. T. K. Thanh, J. Aveyard, and D. G. Fernig, *Anal. Chem.*, 2007, **79**, 4215–21.
- S2. N. G. Khlebtsov, *Anal. Chem.*, 2008, **80**, 6620–6625.
- S3. C. Mätzler, *MATLAB Functions for Mie Scattering and Absorption (research report, University of Bern)*, 2002.
- S4. P. B. Johnson and R. W. Christy, *Phys. Rev. B*, 1972, **6**, 4370–4379.
- S5. X. Liu, M. Atwater, J. Wang, and Q. Huo, *Colloids Surf. B*, 2007, **58**, 3–7.
- S6. N. Nerambourg, R. Praho, M. H. V. Werts, D. Thomas, and M. Blanchard-Desce, *Int. J. Nanotechnol.*, 2008, **5**, 722.
- S7. J. Yguerabide and E. E. Yguerabide, *Anal. Biochem.*, 1998, **262**, 137–156.
- S8. D. D. Evanoff and G. Chumanov, *J. Phys. Chem. B*, 2004, **108**, 13957–13962.